



MATHEMATICAL MODELLING AND ANALYSIS

Volume 24, Issue 4, 494–506, 2019

<https://doi.org/10.3846/mma.2019.030><http://mma.vgtu.lt>

ISSN: 1392-6292

eISSN: 1648-3510

# The Gyrotron Startup Scenario in the Single Mode Time Dependent Approach

Kacper Nowak<sup>a</sup>, Edward Franciszek Plinski<sup>a</sup>,  
Tadeusz Wieckowski<sup>a</sup> and Olgierd Dumbrajs<sup>b</sup>

<sup>a</sup> *Wroclaw University of Technology*

Wybrzeze Wyspianskiego 27, 50-370 Wroclaw, Poland

<sup>b</sup> *University of Latvia*

Raiņa bulvāris 19, LV-1586 Riga, Latvia

E-mail(*corresp.*): [kacper.nowak@pwr.edu.pl](mailto:kacper.nowak@pwr.edu.pl)

E-mail: [edward.plinski@pwr.edu.pl](mailto:edward.plinski@pwr.edu.pl)

E-mail: [tadeusz.wieckowski@pwr.edu.pl](mailto:tadeusz.wieckowski@pwr.edu.pl)

E-mail: [olgertsd@lu.lv](mailto:olgertsd@lu.lv)

Received January 4, 2019; revised June 5, 2019; accepted June 9, 2019

**Abstract.** The paper explains how to solve the Gyrotron equation system in the Single Mode Time Dependent Approach. In particular, we point out problems encountered when solving these well-known equations. The starting current estimation approach a using time model is suggested. The solution has been implemented in the Matlab code, which is attached to the article.

**Keywords:** time dependent approach, gyrotron, differential equation, Matlab code.

**AMS Subject Classification:** 34-04; 34M25.

**Online supplementary material:** Supporting information for this paper is available as online supplementary material at <https://doi.org/10.3846/mma.2019.030>

## 1 Introduction

Gyrotron theory and equations have been well-known since the 80s [7], as well as in more recent times [1,2]. There are papers presenting the results of calculations [11,15]. However, the implementation of the theory is not obvious and the reference data available in the literature usually lacks a few steps, making it impossible to verify and reproduce the results. As a consequence, other researchers are unable to verify their own codes.

In this paper, we document and comment on a way of solving the single mode time dependent equation system. We are focused on the low power

---

Copyright © 2019 The Author(s). Published by VGTU Press

This is an Open Access article distributed under the terms of the Creative Commons Attribution License (<http://creativecommons.org/licenses/by/4.0/>), which permits unrestricted use, distribution, and reproduction in any medium, provided the original author and source are credited.

gyrotrons. In this equation system,  $\tau$  - dimensionless time factor is introduced. It is possible to observe the evolution of the resonator electromagnetic field profile (RF field - starting from the random noise) and its interaction with the electron beam observed as electron momentum change in time and space. The accuracy of this model will be discussed and as is the case with every model, this one also has limitations. Matlab was chosen as the programming environment.

## 2 Time dependent approach formalism

In this paper we have implemented the equation system presented in [1]. This model is often described in the literature as an "old" equation system [13], because it does not take into account two physical effects:

- Dependence of the electron relativistic factor on the axial coordinate.
- Dependence of the magnetic field on the axial coordinate (magnetic field tapering).

These two factors are usually very weak, and can be neglected. Therefore, we have decided that this model is very suitable for the purpose of the article.

In comparison to the self consistent equation system, in this model the time factor  $\tau$  has been introduced.

$$\begin{cases} \frac{d^2 f}{d\zeta^2} - i \frac{df}{d\tau} + \delta f = I \frac{1}{2\pi} \int_0^{2\pi} p d\theta, \\ \frac{dp}{d\zeta} + i(\Delta + |p|^2 - 1)p = if(\zeta, \tau). \end{cases} \quad (2.1)$$

Equation system (2.1) describes the first harmonic and the single mode TE interaction. Variables are normalized according to the formalism used by G. Nusinovich [12].

It is necessary to clarify the meaning of the variables and their naming convention. In Figures 1 and 2 the resonator cross and longitudinal sections, the variable names used in this paper, and the description of each variable are presented. All input, output and intermediate data is organized in groups, and it is therefore easy to see which value is an input parameter, a computed value or expected output parameter.

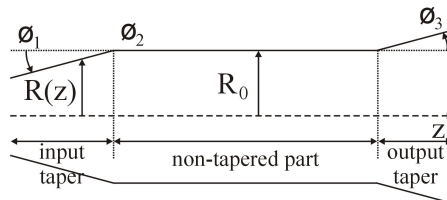
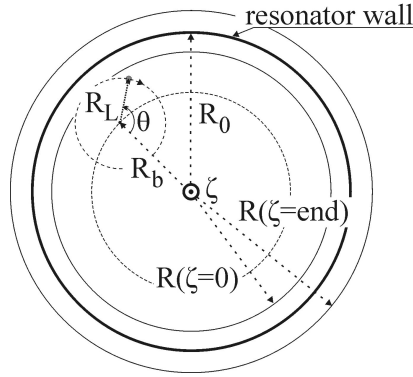


Figure 1. Resonator wall profile along z axis.



**Figure 2.** Resonator cross section.

## 2.1 Physical constants

To reproduce results it is mandatory to use the same accuracy and value of all physical constants. The following values are used and the reader should pay attention to units and dimensions:

- $c$  – light velocity =  $299.792458 \left[ \frac{mm}{ns} \right]$ , because we use a frequency in GHz and  $\left[ \frac{1}{ns} = 1GHz \right]$ ;
- $m_e$  – electron mass =  $9.109382914e-13 \left[ \frac{kV \cdot A \cdot ns^3}{mm^2} \right]$  – electron rest mass;
- $e$  – electron charge =  $1.602176620898e-10 \left[ A \cdot ns \right]$  electron charge;
- $\mu$  – permeability =  $1.2566370614e-3 \left[ \frac{kV \cdot ns}{A \cdot mm} \right]$  vacuum permeability;
- $\epsilon$  – permittivity =  $8.854188e-3 \left[ \frac{F}{mm} = \frac{A \cdot ns}{kV \cdot mm} \right]$  vacuum permittivity.

## 2.2 Input variables

To begin calculations in the time domain, the values of some variables need to be assumed. These are resonator dimensions, the number of electrons in the simulation, mode numbers  $mandk$ , the harmonic number, and cathode voltage. The remaining variables can be estimated using the Cold Cavity Method (optimal frequency and diffraction factor) or with the Self-Consistent Method (direction of mode rotation, beam current) [5]. The two approaches mentioned above are not considered in this article. The most efficient direction of mode rotation can be found in the time domain calculations by calculating coupling coefficients. It does not need to be inputted, but we will assume the direction of mode rotation a priori, because we want to show that it is possible and correct to simulate the chosen direction of mode rotation, which is not necessarily the most efficient one (e.g. in the multimode, time dependent mode competition case). The following needs to be known in order to solve time domain equation system (2.1):

- $m, k$  – chosen azimuthal and radial mode numbers;

- $z$  – axis vector, includes the tapered part of the resonator and defines a spacial dimension in the simulation;
- $\alpha = \frac{V_{\perp}}{V_{\parallel}} = \frac{\beta_{\perp}}{\beta_{\parallel}}$  – pitch factor (orbital to axial velocity ratio), determined by the magnetic field shape, gun shape and distance between the resonator and gun. Its value is usually between 1.2 and 1.5 at the resonator interaction space. A low value means that there is less energy parallel to the electric field to extract, and the high value increases the risk of the magnetic mirror, when electrons will not have enough momentum to reach the collector;
- $R(z)$  – resonator radius vector, wall profile including the tapered part, defined as length if each part  $L = [L_1; L_2; L_3]$  [mm] and angle  $\phi = [\phi_1; \phi_2; \phi_3]$  [radian];
- $R_0$  – resonator radius in the parallel wall; the middle, non-tapered part of the resonator. The electron vs. RF field interaction mainly takes place in this part;
- $B_0$  – magnetic field in the parallel, middle, non-tapered part of the resonator;
- $f_0$  – initial RF field profile vector. The length of this vector is equal to the length of the  $\zeta$  axis. In our case, we assume that there is only white noise in the resonator at the beginning. It is possible to use the cold cavity RF field profile as the initial value in order, to reach the final solution faster. It does not matter what the value of the RF field profile is in the beginning, and the solution should always be converged to the same result;
- $freq_{opt}$  – optimal frequency of the RF field for the chosen resonator design. This parameter is found using the Cold Cavity Theory model (e.g. equation (1) in [4]);
- $mnSign$  –  $\pm 1$  sign that corresponds to the co-rotating mode or counter-rotating mode. It is more probable that the mode with higher energy transfer will appear in a real device, so it is common practice to check the efficiency for both rotations, by calculating the beam-field coupling coefficient  $J_{m\pm n}^2(\nu_{m,k} \cdot R_b/R_0)$  [9]. A higher value of the coupling means that a more probable mode will appear;
- $N_{el}$  – number of electrons used in the simulation. Larger values will lead to better averaging (over the initial electron phase), but will take more computation time. A value between 12-36 is a good choice to start, but it is important to note that to estimate gyrotron efficiency more accurately 256 or more electrons should be used;
- $n = 1$  – harmonic number, in this paper it is assumed to be equal to 1;
- $U_c$  – cathode, electron accelerating voltage. Correspond to the electron kinetic energy;

- $I_c$  – cathode/beam (GUN) current [A]. If it is below the startup current there will be no oscillations – no output power will be observed. With iterative changing of this value it is possible to determine the starting current for the chosen working point.

### 2.3 Intermediate variables

The following intermediate computation steps are required to solve the problem, and therefore all the variables calculated in this solution are presented together:

- $\nu_{m,k}$  – characteristic value, defined as the k-th zero of  $(J'_m)$  – the first derivative of the Bessel m-th order function of the first kind, in other words this is the k-th extreme of the Bessel m-th order function of the first kind;
- $\omega = 2\pi \cdot freq_{opt}$  – optimum angular frequency of the RF field for the chosen resonator design;
- $\omega_{cut} = c \cdot \nu_{m,k}/R_0$  – cutoff angular frequency in the non-tapered resonator part;
- $\omega_{cut}(z) = c \cdot \nu_{m,k}/R(z)$  – cutoff angular frequency as the function of the z axis vector, in the whole resonator including the tapered part;
- $\beta_{\perp} = V_{\perp}/c = \sqrt{\frac{\gamma^2 - 1}{1 + 1/a^2}}/\gamma$  – normalized electron perpendicular velocity;
- $\beta_{\parallel} = \frac{V_{\parallel}}{c} = \sqrt{1 - \frac{1}{\gamma^2} - \beta_{\perp}^2}$  – normalized electron parallel velocity;
- $\omega_{cyc} = \frac{eB_0}{m_e\gamma}$  – electron cyclotron frequency;
- $\zeta = \frac{\beta_{\perp}^2 \cdot \omega}{2 \cdot \beta_{\parallel} \cdot c} \cdot z$  – normalized/dimensionless longitudinal coordinate z, including the tapered part;
- $R_b = \frac{\nu_{m \pm n, 1} \cdot c}{2\pi \cdot freq_{opt}}$  – electron beam radius, when the interaction (energy exchange) between the electric field and electron momentum is highest.  $\nu_{m \pm n, 1}$  is the first root of  $(J'_{m \pm n})$  the derivative of  $m \pm n$  order Bessel function of the first kind, in other words the first extreme of the  $m \pm n$  order Bessel function of the first kind;
- $\delta(z) = \frac{8 \cdot (\beta_{\parallel})^2 \cdot (\beta_{\perp})^{-4}}{\omega_{cyc}} \cdot (\omega_{cut} - \omega_{cut}(z))$  – normalized frequency mismatch – describes variation of the critical frequency along the resonator axis;
- $k_{zend} = \frac{2 \cdot c \cdot \beta_{\parallel} \cdot \beta_{\perp}^{-2}}{\omega_{cyc}} \cdot \sqrt{\frac{\nu_{m,k}^2}{R_0^2} - \frac{\nu_{m,k}^2}{R_{end}^2}}$  – wave factor at the end of the resonator;
- $I_{cn} = I_c \cdot (3.76e^{-3}) \cdot \beta_{\parallel} \cdot \beta_{\perp}^{-6} \cdot \frac{J_{m \pm n}^2(\frac{\nu_{m,k} \cdot R_b}{R_0})}{4\gamma \cdot J_m^2(\nu_{m,k}) \cdot (\nu_{m,k}^2 - m^2)}$  – normalized beam current;
- $\Delta = (\frac{2}{\beta_{\perp}^2}) \cdot \frac{\omega - n \cdot \omega_{cyc}}{\omega_{cyc}}$  – normalized cyclotron frequency mismatch ([6]);

- $\eta_{el} = \frac{(1+\gamma) \cdot \alpha^2}{2 \cdot \gamma \cdot (1+\alpha^2)}$  – electron compression efficiency. This factor is correlated to the perpendicular and parallel velocity ratio at the gun area and at the resonator interaction space (Figure 3);
- $\tau = \frac{\beta_{\perp}^4 \cdot \omega_{cyc}}{8 \cdot \beta_{\parallel}^2} \cdot t$  – normalized/dimensionless time.

### 2.4 Output variables

The following information is expected to be obtained as a result of the computation:

- $\tau, \zeta$  – normalized time and z axis;
- $f(\tau, \zeta)$  – RF field evolution in time over zeta axis;
- $\eta_{gyro}(\tau)$  – gyrotron total efficiency evolution in time;
- $P_{out}(\tau)$  – gyrotron output power evolution in time.

## 3 The solution

To solve the equation system (2.1) it is necessary to assume the initial conditions and one boundary condition, or two point boundary condition for each equation.

### 3.1 Initial conditions

- *RF field equation.* At the beginning, before the gun is powered, there is only noise inside the resonator. Therefore, as the initial condition for the field equation one can assume white noise  $f_0(\zeta) = 0.1 \cdot e^{<0 \div 2\pi i>}$  at time  $\tau = 0$  for all  $\zeta$ .
- *Electron momentum equation.* Electrons are gyrating along magnetic field lines and are moving forward along the z axis. Electrons are gyrating with Larmor radius  $R_L$  and the center of the gyration trajectory is displaced from the center of the resonator by radius  $R_b$ . The initial condition for the electron momentum equation describes where the electron enters the resonator space. In Figure 2, the initial (when entering the resonator space,  $\zeta = 0$ ) gyration phase  $\theta$  is marked. The electron initial phase is random, so for the simulation one can assume that  $\theta$  are equally spaced in the range  $< 0 \div 2\pi >$  (3.1) and average over  $\theta$ . More electrons will lead to better averaging, and a number between 12 and 48 can be seen as a good choice.

$$P_0 = e^{i \cdot \theta}, \theta \in < 0 \div 2\pi >, \tag{3.1}$$

$P_0$  – the equally distributed vector of complex numbers with a length equal to the number of electrons in the simulation.

### 3.2 Boundary conditions

Wave propagating in the resonator is supposed to be entirely reflected on the electron input side of the resonator  $\zeta = 0$  and fully transferred on the output side of the resonator  $\zeta = end$ , the so-called reflection-less boundary condition. If the wave is not reflected entirely at the input it may cause interaction with electrons that have not yet reached the resonator space and the operation will be disturbed. Unwanted oscillations in the GUN area are especially studied in high power gyrotrons [3]. The literature proposes other kinds of boundary condition for the radiation of the Fourier components of the RF field of Robin's type, which are discussed in [2]. In this work we use the reflection-less boundary condition.

The value of the field at the input of the resonator should drop to 0 (3.2), and at the output the reflection-less boundary condition is applied (3.3).

$$f(\zeta = 0, \tau) = 0, \quad (3.2)$$

$$f(\zeta, \tau) + \frac{1}{\sqrt{\pi i}} \int_0^\tau \frac{1}{\sqrt{\tau - \tau'}} \frac{df(\zeta, \tau')}{d\zeta} d\tau' \Big|_{\zeta=end} = 0. \quad (3.3)$$

Equation (3.3) in the steady state can be replaced with equation (3.4).

$$f(\zeta, \tau) = \frac{i}{k} \frac{df(\zeta, \tau)}{d\zeta} \Big|_{\zeta=end}, \quad (3.4)$$

where  $k = 2c\beta_\perp\beta_\parallel^{-2}\omega_{cyc}^{-1}(\omega_{cut}^2/c^2 - \nu^2/R^2(\zeta = end))^{1/2}$ .

### 3.3 Matlab first and second order derivative solver

The solution is found iteratively. First the electron motion equation for  $p$  is solved by supplying the initial field value (white noise or RF field profile from cold cavity calculations) into the equation system (2.1). When  $p$  is calculated for a very small step of time  $\tau$  and all space steps  $\zeta$ , then integral  $\langle p \rangle$  is used to find  $f$  in (2.1). Thus, the RF field is updated for every temporal step after electrons pass. A passing particle "does not see" the effect of the disturbance it is causing in the electric field. Only the following electrons (on the next  $\langle p \rangle$  update step) are affected by the changed RF field. Therefore, condition  $T_{decay}$  of the electric field  $\gg T_{transit}$  of the electrons must hold in this model.

#### 3.3.1 Solving the electron momentum equation

To solve the electron momentum equation, the "ode45" Matlab solver can be used. Equation  $\frac{dp}{d\zeta} + i(\Delta + |p|^2 - 1) \cdot (p/n) = i \cdot p^{n-1} f(\zeta, \tau)$  can be rewritten as follows

$$\frac{dp}{d\zeta} = i \cdot f(\zeta) \cdot p^{(n-1)} - i \cdot (p/n) \cdot (\Delta + |p|^2 - 1), \quad (3.5)$$

which makes it possible to implement in the Matlab solver.

The "ode45" solver takes as an argument the definition of the function that calculates and returns  $\frac{dp}{d\zeta}$ . This function is implementing equation (3.5)

and needs the following arguments: RF field  $f(\zeta)$ , longitudinal coordinate  $\zeta$ , cyclotron frequency mismatch  $\Delta$ , harmonic number  $n = 1$ .

When the above equation is solved for each initial condition  $\theta$ , then the integral over  $\theta$  for the current time  $\tau$  has to be calculated and averaged

$$\langle p \rangle = \left[ \int_0^{2\pi} P(\zeta, \tau) d\theta \right] \cdot \frac{1}{2\pi}. \tag{3.6}$$

This integral is needed to compute the RF field for the next temporal step  $\tau$ .

To estimate output power and the gyrotron efficiency, the integral for  $\zeta$  at the exit from the resonator has to be calculated

$$\left[ \int_0^{2\pi} |P(\zeta, \tau)|^2 d\theta \right] \cdot \frac{1}{2\pi} \Big|_{\zeta=end}.$$

The calculated integrals of the electron momentum enable the efficiency and output power at each time step  $\tau$  to be estimated. The following equations have to be solved:

- Electron perpendicular efficiency –  $\eta_{\perp}(\tau) = 1 - \frac{1}{2\pi} \cdot \int_0^{2\pi} P^2(\zeta\tau) d\theta \Big|_{\zeta=end}$ . This factor is the efficiency of energy transfer from the electron kinetic energy to the RF field in the cyclotron resonance mechanism;
- Total efficiency –  $\eta_{gyro}(\tau) = \eta_{\perp}(\tau) \cdot \eta_{el}$  (see Figure 3);

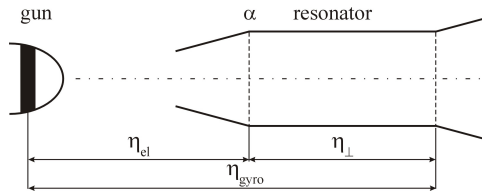


**Figure 3.** Electron compression  $\eta_{el}$ , interaction  $\eta_{\perp}$ , gyrotron total  $\eta_{gyro}$  efficiencies.

- Gyrotron output power –  $M(\tau) = I_c \cdot U_c \cdot \eta_{\perp}(\tau) \cdot \eta_{el}$ .

Electron efficiency  $\eta_{el}$  describes how much total electron energy is converted to the perpendicular kinetic energy (perpendicular velocity). Only this energy can be transferred to the RF field by the electron and the electric field interaction mechanism. Variable  $\eta_{\perp}(\tau)$  describes the efficiency of the energy transfer from the electron momentum to the electric field. It is called perpendicular (to axis  $\zeta$ ) because only the perpendicular part of the electron velocity (momentum) is important in the interaction with electric field vector  $E$ , which is also perpendicular to  $\zeta$  axis.

At this point the electric field profile for the next time step  $\tau + 1$  can be calculated. The RF field was changed by interaction with the electrons passing through the resonator, so it must be recalculated using a new  $\langle p \rangle$  value.



### 3.3.2 Solving the electric field profile equation

To solve the Schrodinger type linear partial differential field equation, the second order differential equation solver has to be used. In paper [13], the method of lines [8] with the "ode15s" solver was proposed. However, Matlab offers the "pdepe" function, which implements the second order algorithm that we have employed to find the solution. The electrons impact on the RF field is noted as integral (3.6) which is one of the parameters supplemented to  $f(\zeta)$  in equation system (2.1). Equation

$$\frac{d^2 f(\zeta, \tau)}{d\zeta^2} - i \frac{df(\zeta, \tau)}{d\tau} + \delta(\zeta, \tau) f(\zeta, \tau) = I_{cn} \frac{1}{2\pi} \int_0^{2\pi} p(\zeta, \tau) d\theta$$

has to be transformed to a form acceptable for the Matlab "pdepe" solver [14]:

$$c(x, t, u, \frac{du}{dt}) = x^{-m} \frac{d}{dx} (x^m f(x, t, u, \frac{du}{dx})) + s(x, t, u, \frac{du}{dx}), \tag{3.7}$$

which in the considered case of Equation (2.1) takes the form:

$$i \frac{df(\zeta, \tau)}{d\tau} = \frac{d^2 f(\zeta, \tau)}{d\zeta^2} + \delta(\zeta, \tau) f(\zeta, \tau) - I_{cn} \frac{1}{2\pi} \int_0^{2\pi} p(\zeta, \tau) d\theta.$$

When comparing the RF field in equation (2.1) with Matlab manual equation (3.7), the convention is:  $\zeta \Leftrightarrow x, f \Leftrightarrow u, \tau \Leftrightarrow t$ . For this reason, the parameters supplied for the "pdepe" "pdefun" solver function are:

- $c(x, t, u, \frac{\delta u}{\delta t}) \Rightarrow 1i$ ;
- $x^{-m} \frac{\delta}{\delta x} (x^m f(x, t, u, \frac{\delta u}{\delta x}))$  for  $m = 0 \Rightarrow f = x^{-0} \frac{\delta}{\delta x} (x^0 \frac{\delta u}{\delta x}) \Rightarrow f = \frac{\delta u}{\delta x}$ ;
- $s(x, t, u, \frac{\delta u}{\delta x}) \Rightarrow s = \delta(x, t)u - I_{cn} \frac{1}{2\pi} \int_0^{2\pi} p(x, t) d\theta$ .

To use the "pdepe" solver, the temporal axis must be normalized and boundary condition (at resonator input  $\zeta = 0$  and output  $\zeta = end$ ) equations (3.2) and (3.4) must be supplied. Boundary conditions in the Matlab are defined as function "bcfun" which has the form of

$$p(x, t, u) + q(x, t) f(x, t, u, \frac{du}{dx}) = 0.$$

In the case of the considered equations, "bcfun" takes as the input the estimated value of the RF field function at the left and right boundaries and returns vectors  $q$  and  $p$  factors at the left and right boundary (as described in the Matlab "pdepe" manual).

Initial conditions ( $f$  for  $\tau = 0$ ) must also be supplied. In the Matlab convention, the function supplying initial conditions "icfun" takes the form  $u(x, t_0) = u_0(x) \Rightarrow u_0(x) \Leftrightarrow f_0(\zeta) = 0.1e^{<0 \pm 2\pi i>}$ . In other words, the initial RF field can be supplied as a white noise or as some other predefined RF field. In multi-mode time dependent calculations initiated by predefined field profile it should be possible to simulate the inputting external field in order to favor a certain mode in the resonator.

### 3.3.3 Solving the equation system

To solve equation system (2.1) in the first iteration  $f_{t=0}$  the initial RF field value (random noise) is input to the electron momentum equation. Then the integral  $\langle p \rangle_{t=0}$  is calculated and used as the input to the RF field equation. It is assumed that the time step is equal to 0.05 [ns]. The new RF field profile  $f_{t=0.05}$  is calculated and then used as the input into the electron motion equation. Integral  $\langle p \rangle_{t=0.05}$  is supplied to the RF field equation together with  $f_{t=0.05}(\zeta)$  (field from previous iteration) as the initial condition for the pdepe solver. As a result,  $f_{t=0.1}(\zeta)$  is obtained. The algorithm is then iterated until the chosen final time  $t = end$ .

## 4 Results

This section presents all the input, intermediate and output data, that is usually omitted in literature. Therefore, these results can be used as comparison data for the other researchers to verify their own codes at each crucial step of the simulation.

Sample calculations were made for the following resonator: mode  $TE_{0,1}$ ,  $n = 1$ ,  $R_0 = 7.5[mm]$ ,  $R(z)$  expressed as  $L = [30; 70.9; 30]$ ,  $\phi = [2.3; 0; 3]$ ,  $\alpha = 1.4$ ,  $U_c = 12[kV]$ ,  $I_c = 0.27[A]$ ,  $freq_{opt} = 24.43894431[GHz]$ ,  $N_{el} = 24$ ,  $B_0 = 0.87878[T]$ .

It is assumed that spacial step 0.05 [mm] is sufficient for accurate calculations. The input data provided above are sufficient to carry out time dependent calculations.

The most important intermediate data is listed below, and some variables were omitted as their importance is not crucial:  $\nu_{0,1} \cong 3.832$ ,  $mnSign = +1$ ,  $\omega_{cut} \cong 153.16[\frac{1}{GHz}]$ ,  $\omega_{cyc} \cong 151.01[\frac{1}{GHz}]$ ,  $\gamma \cong 1.0235$ ,  $\beta_{\perp} \cong 0.1733$ ,  $\beta_{\parallel} \cong 0.1238$ ,  $R_b \cong 3.595[mm]$ ,  $k_{z_{end}} \cong 4.7037$ ,  $\Delta \cong 0.9467$ .

The final results are presented in Figures 4–5.

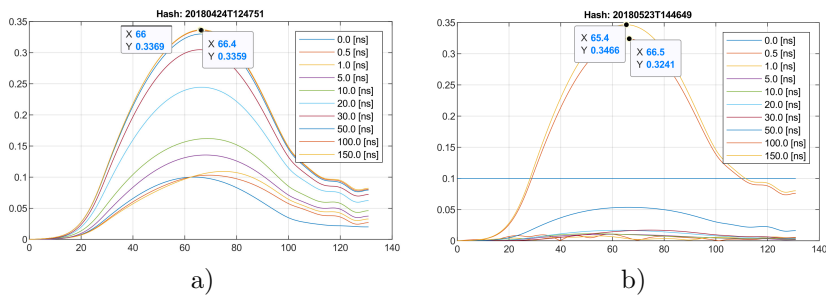


**Figure 4.** RF field energy as a function of  $z$  – temporal evolution, starting from: a) the cold cavity field, b) white noise.

The RF field temporal evolution shown in Figure 4a was obtained from the cold cavity approximation for the initial RF field value. Similar results, obtained by using white noise as the initial condition, are shown in Figure 4b.

The difference is in the computation time. It takes longer for the field to form starting from the white noise initial condition.

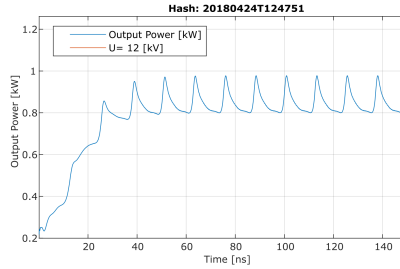


**Figure 5.** Gyrotron output power in the time domain.

Output power simulation in the single mode approach is useful to check using non-linear theory, which working point the gyrotron will finally reach. If the beam current is too low then the RF field will collapse and output power will not raise, or will drop to zero quickly (Figure 6). There is a risk involved in using the Runge-Kutta 4-th order algorithm that one should be aware of. When the RK4 plain procedure was employed to solve the electron momentum equation, output power did not drop to zero when the beam current was very low (below startup current). The power was dropping to some constant level, which is obviously a flaw. Applying Matlab "ode45" (RK4 with 5-th order error verification) solved this numerical problem and the results have become reliable. It has been verified that using the Time dependent approach allows one to simulate the time evolution of the RF field and power. Seeing an animation reaches peoples' imagination. Therefore, in our opinion this model is a very good tool to get engineering intuition about the gyrotron startup. The authors were unable to determine if the oscillations in Figure 5 are the result of the numeric procedures.

#### 4.1 Starting current estimation in time dependent theorem.

Starting current estimation can be done in a classic way [4, 10], but it can also be found by iterating the time simulation for different beam current values until stable power at the output and a stable RF field can be observed. This is quite a convenient method as it does not need extra programming, but it does require computation time. The simulation has to be long enough to observe a steady state, and not a temporary result. Start current estimation is presented in Figure 6. The value of the starting current is in the range 0.17–0.18 [A].

## 5 Conclusions

Time dependent simulation is quite tricky, as solving differential equations always leads to "some" results, but not necessary to good ones. Therefore, it is very important to verify calculated results, but it is not so obvious of how to do it as there is no pattern for comparison. The first thing that a researcher can

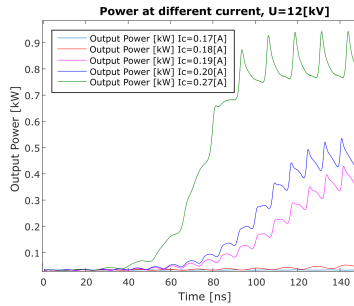


**Figure 6.** Gyrotron output power for different current value.

do is use some engineering intuition, and to carefully observe shapes, values and units. In the case of the RF field it is good to check if the equation will lead to the same result regardless of the startup condition, which can be seen when comparing both plots in Figure 4. It is good to try some well-know conditions, where the result can be expected. For example, if the electron current is chosen below the startup current, then one would obviously expect no oscillation. It is good to check this by using different solvers for the differential equation. In this case, "ode45" is a Matlab solver, but a simple Runge-Kutta 4 order solver can be easily implemented and tested too. Another case is the optimization that leads to the final results. It is important to remember that the optimal solution should be found within the search range and not at the edge of the range. Another option is to use commercial simulation software (like PIC code) and compare the result or ask other researchers to verify your results against their code and knowledge. However, to do this it is required to share all data, especially the intermediate data that is very helpful in debugging equations and codes.

One flaw that the authors of this paper know about and have failed to find the source of output power oscillation. It is assumed that the cause is numeric based and not physics based, but this case is yet to be resolved.

In this paper, the results have been presented as a movie, and the Matlab source code is also included. The attached files include all the data (high precision) required to reproduce our results.

## References

- [1] M.I. Airila, O. Dumbrajs, A. Reinfelds and U. Strautiņš. Nonstationary oscillations in gyrotrons. *Physics of Plasmas*, **8**(10):4608–4612, 2001. <https://doi.org/10.1063/1.1402173>.
- [2] J. Cepitis, O. Dumbrajs, H. Kalis, A. Reinfelds and U. Strautins. Analysis of equations arising in gyrotron theory. *Nonlinear Analysis: Modeling and Control*, **17**(2):139–152, 2012.
- [3] A.J. Cerfon, E. Choi and C.D. Marchewka et al. Observation and study of low-frequency oscillations in a 1.5-MW 110-GHz gy-

- rotron. *IEEE Transactions on Plasma Science*, **37**(7):1219–1224, 2009. <https://doi.org/10.1109/TPS.2009.2020903>.
- [4] O. Dumbrajs, T. Idehara, T. Saito and Y. Tatematsu. Calculations of starting currents and frequencies in frequency-tunable gyrotrons. *Japanese Journal of Applied Physics*, **51**:126601, 2012. <https://doi.org/10.1143/JJAP.51.126601>.
- [5] O. Dumbrajs and G.S. Nusinovich. Cold-cavity and self-consistent approaches in the theory of mode competition in gyrotrons. *IEEE Transactions on Plasma Science*, **20**(3):133–138, 1992. <https://doi.org/10.1109/27.142812>.
- [6] N.S. Ginzburg, G.S. Nusinovich and N.A. Zavolsky. Theory of non-stationary processes in gyrotrons with low Q resonators. *International Journal of Electronics*, **61**(6):881–894, 1986. <https://doi.org/10.1080/00207218608920927>.
- [7] N.S. Ginzburg, N.A. Zavolskii, G.S. Nusinovich and A.S. Sergeev. Onset of self-oscillations in electronic microwave oscillators with diffraction radiation output. *Radiofizika*, **29**:106–114, 1986.
- [8] S. Hamdi, W.E. Schiesser and G.W. Griffiths. Method of lines. *Scholarpedia*, **2**(7):2859, 2007. <https://doi.org/10.4249/scholarpedia.2859>.
- [9] T. Idehara, J.C. Mudiganti and L. Agus et al. Development of a compact sub-THz gyrotron FU CW CI for application to high power THz technologies. *Journal of Infrared, Millimeter, and Terahertz Waves*, **33**(7):724–744, 2012. <https://doi.org/10.1007/s10762-012-9911-0>.
- [10] H. Khatun, R.R. Rao, A.K. Sinha and S.N. Joshi. Accurate estimation of start oscillation current for maximum output power in 42 GHz, 200 kW gyrotron. *Indian J. Pure Ap. Phy.*, **49**:776–781, 2011.
- [11] T. Numakura, T. Imai, T. Kariya and et al. Code development for the calculations of time-dependent multimode oscillations in the cavity of the future high-power gyrotrons. In *AIP Conference Proceedings*, 030023, 2016.
- [12] G.S. Nusinovich. *Introduction to the Physics of Gyrotrons*. JHU Press, 2004.
- [13] A. Reinfelds, O. Dumbrajs, H. Kalis, J. Cepitis and D. Constantinescu. Numerical experiments with single mode gyrotron equations. *Mathematical Modelling and Analysis*, **17**(2):251–270, 2012. <https://doi.org/10.3846/13926292.2012.662659>.
- [14] Inc. The MathWorks. Matlab manual. Online, 2006. Available from Internet: <https://www.mathworks.com/help/matlab/ref/pdepe.html>.
- [15] A.Q. Zhao, B.S. Yu and C.T. Zhang. Startup and mode competition in a 420 GHz gyrotron. *Physics of Plasmas*, **24**(9):093102, 2017. <https://doi.org/10.1063/1.4997910>.